



Institut national
de la santé et de la recherche médicale

Actualités en IRM thoracique

Damien Mandry

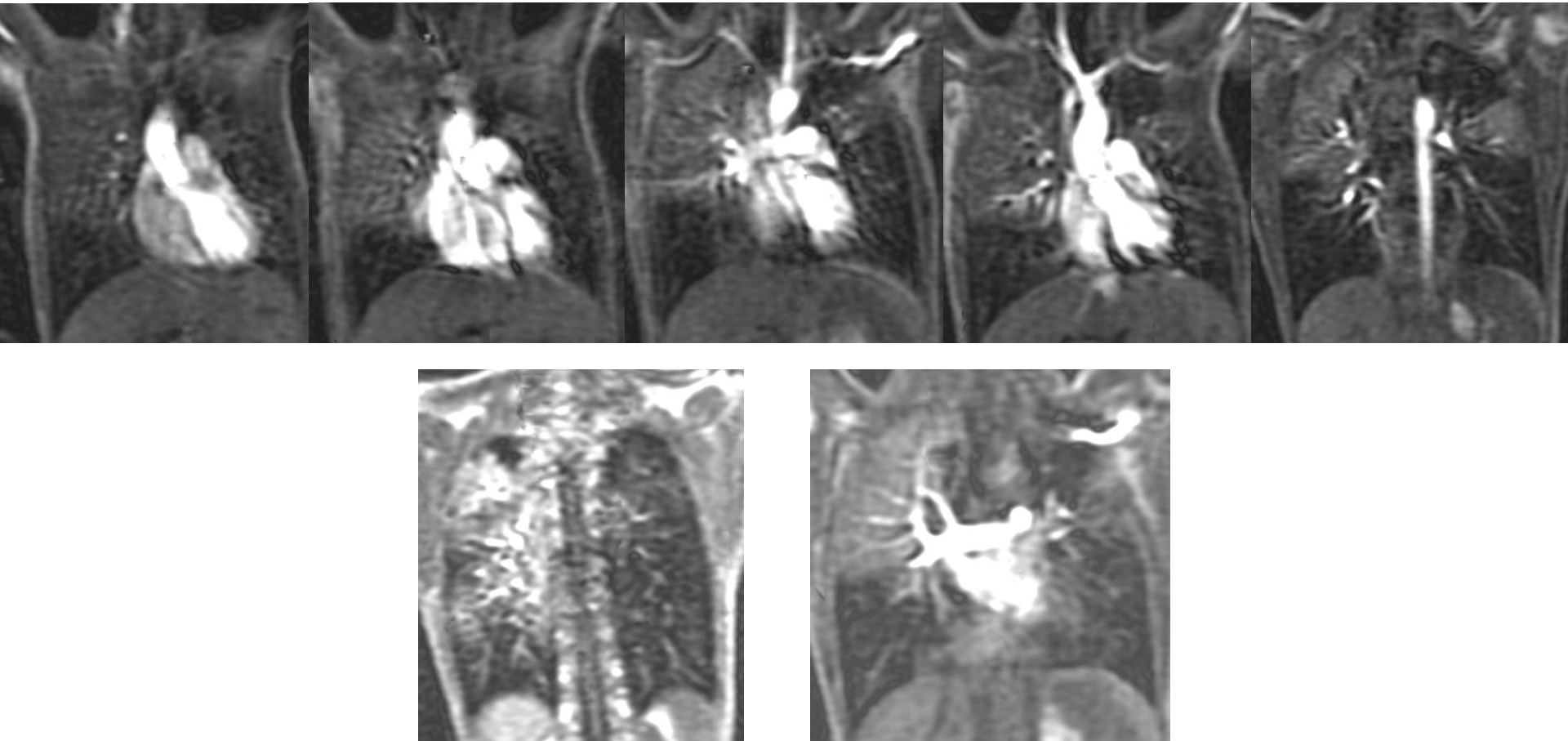


Principes physiques

- **Champ magnétique** intense
 - 1.5 Tesla \leftrightarrow 30000 x champ magnétique terrestre
 - D'où les CI
- **3 grandeurs** caractérisent les tissus biologiques
 - Densité de protons
 - T1
 - T2 (env. 10x plus court que le T1)
- **Pondération** d'une séquence \leftrightarrow privilégier l'une de ces grandeurs
=> distinction des \neq tissus (**caractérisation** lésionnelle)

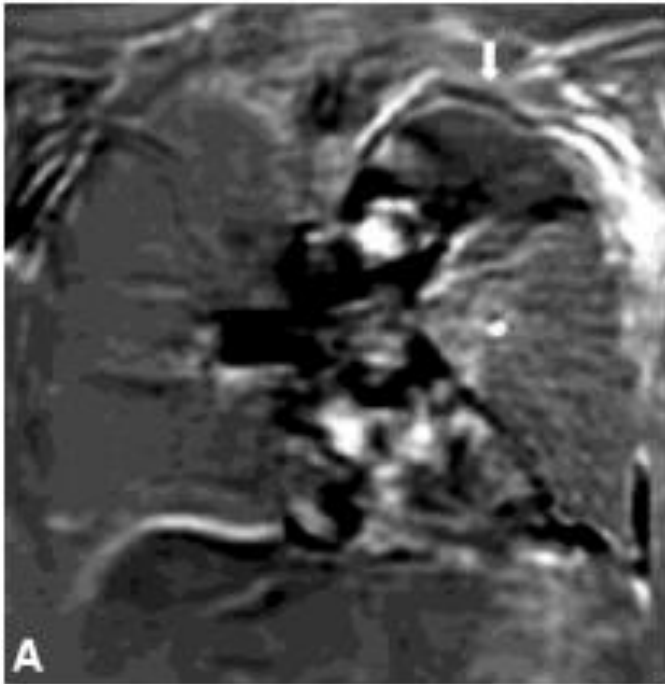
IRM : perfusion

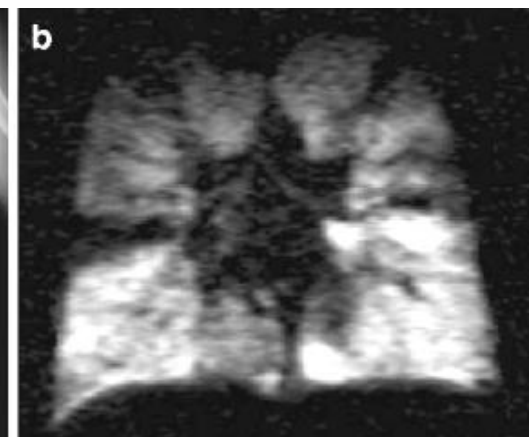
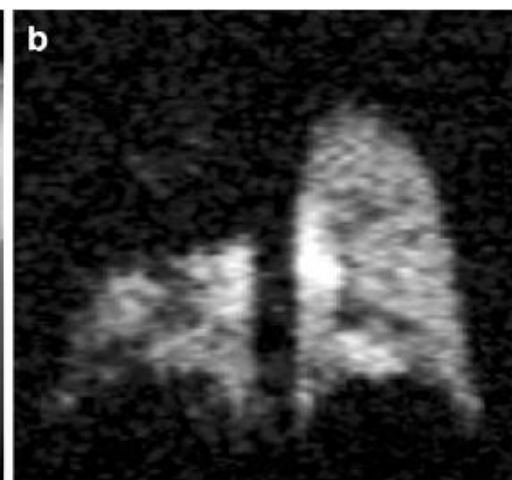
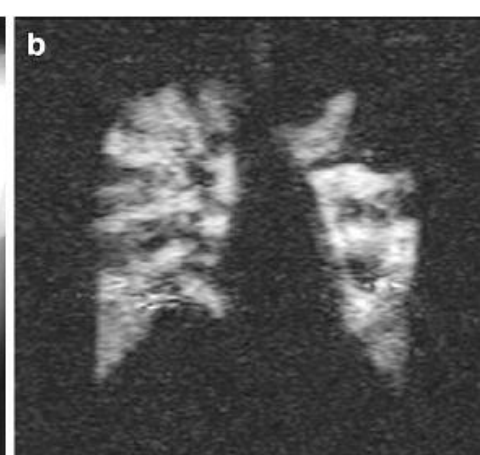
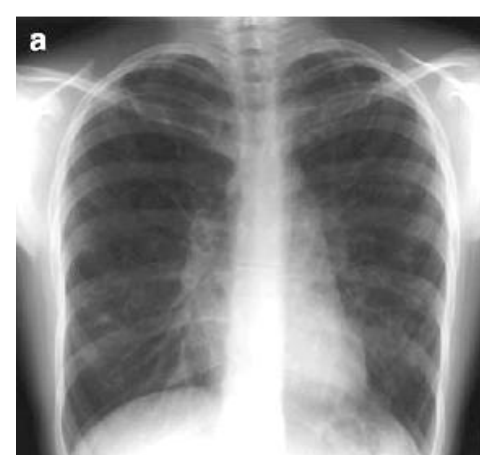
- Séquences en EG T1 après injection de chélate de Gd
 - Eichinger M et al. Contrast-enhanced 3D MRI of lung perfusion in children with cystic fibrosis. Eur Radiol 2006; 116:2147-2152



IRM : ventilation

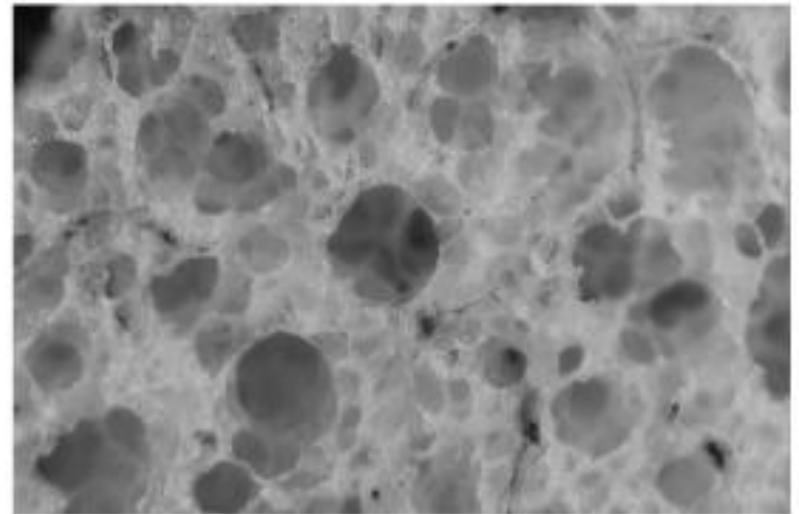
- Jakob PM et al. Assessment of human pulmonary function using oxygen-enhanced T1 imaging in patients with cystic fibrosis. Magn Reson Med 2004; 51:1009-1016
- McMahon CJ et al. Hyperpolarized (3)helium magnetic resonance ventilation imaging of the lung in cystic fibrosis: comparison with HRCT and spirometry. Eur Radiol 2006
- Van Beek EJR et al. Assessment of lung disease in children with cystic fibrosis using hyperpolarized 3-He MRI: comparison with Shwachman score, Crispin-Norman score and spirometry. Eur Radiol 2006





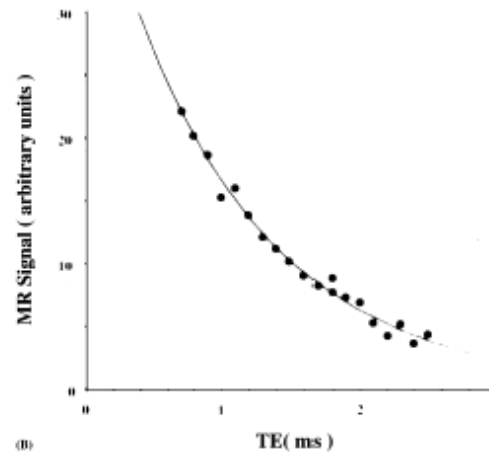
Evaluation du parenchyme

- Physiologie pulmonaire :
 - Contient environ 300 millions d' alvéoles
 - Mesurant 200 à 300 μm de diamètre
 - Et représentant une surface globale de 50 à 70 m^2
 - Densité moyenne
 - 0,3 g/mL en fin d' expiration
 - 0,15 g/mL en fin d' inspiration
 - Ventilation = 6 L/min au repos



Poumon et signal IRM

- Faible signal RMN
 - Architecture alvéolaire, avec de multiples interfaces air - tissu
 - Hétérogénéités +++ par susceptibilité magnétique
 - T2* très court (1,4 msec)
 - Faible densité protonique
 - Perte de signal en raison des mouvements cardiaques et respiratoires, du flux sanguin pulmonaire et de la diffusion moléculaire



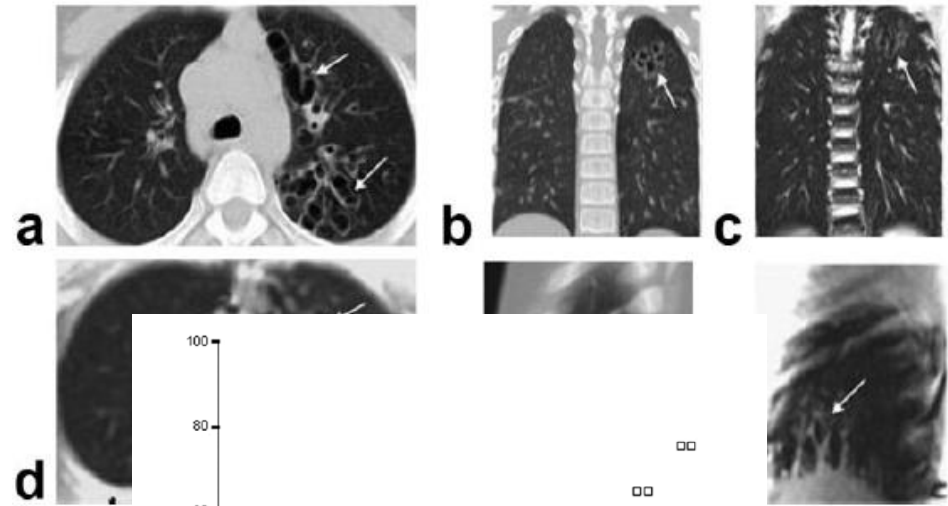
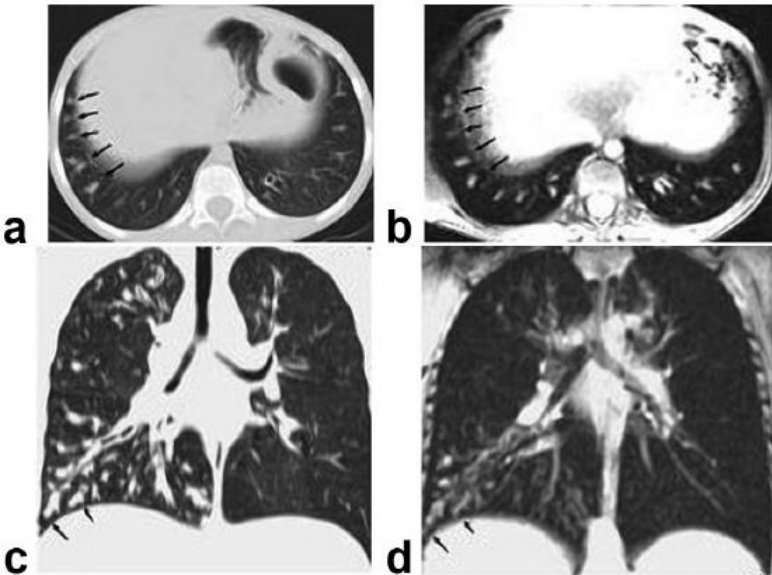
$T2^* = 1,03 \text{ msec}$; densité relative de protons = 0,36

$$SI = D \cdot e^{-TE/T2^*}$$

Utiliser des séquences à TE très court +++

Mucoviscidose

- Motivations
 - Irradiation
 - Suivi ++
 - Distribution, étendue et importance des lésions facilitant le diagnostic

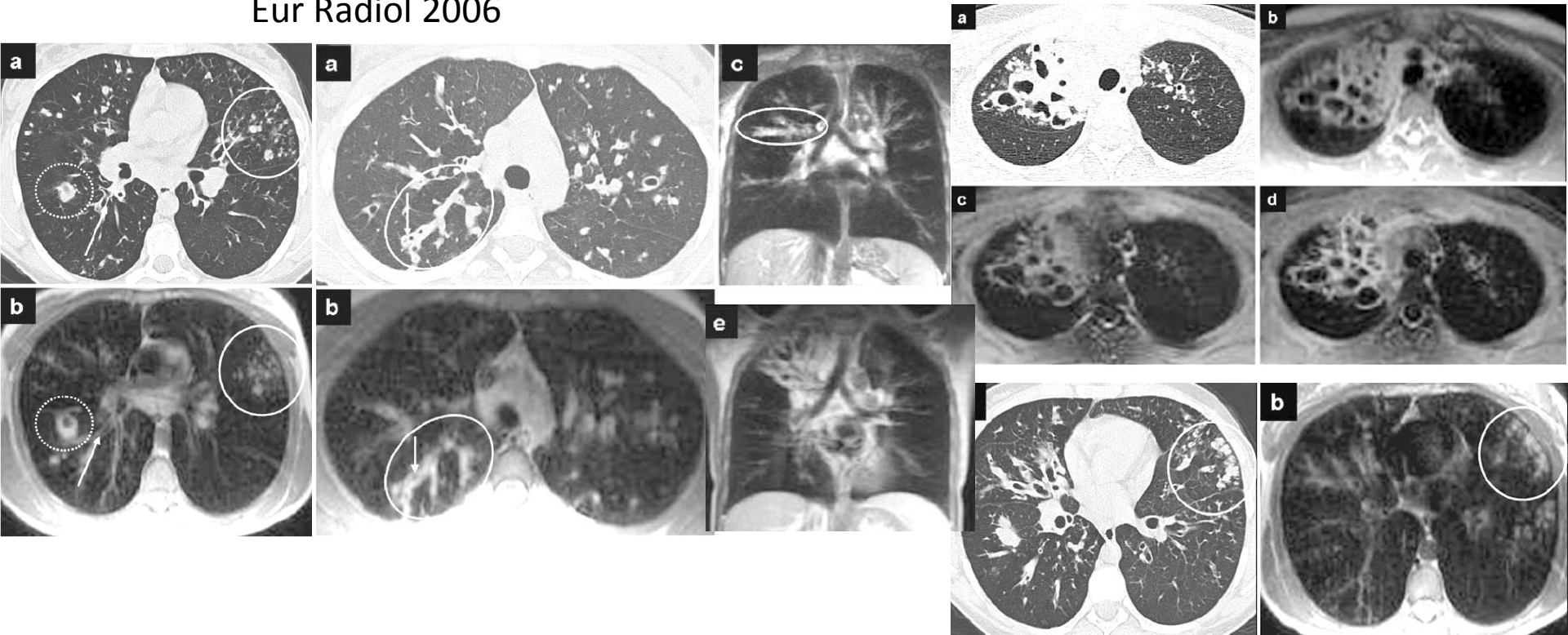


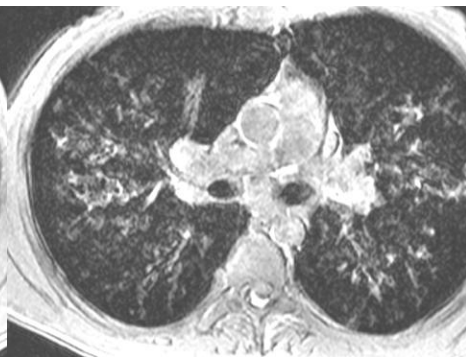
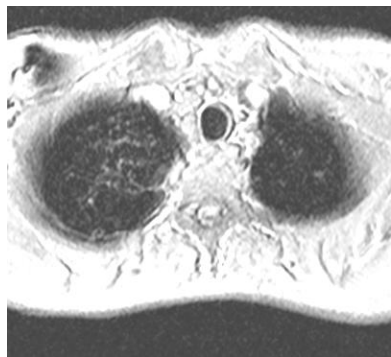
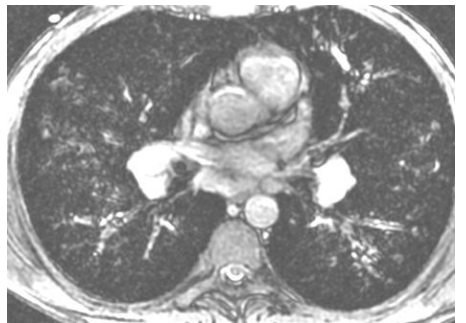
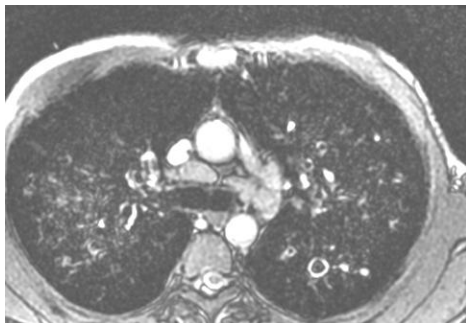
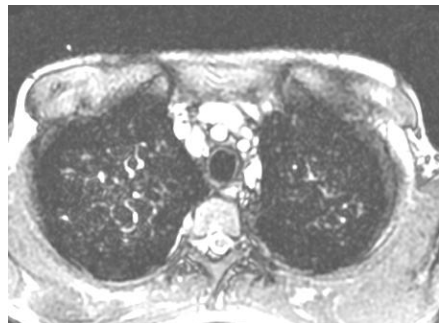
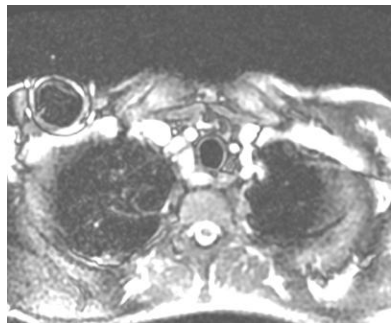
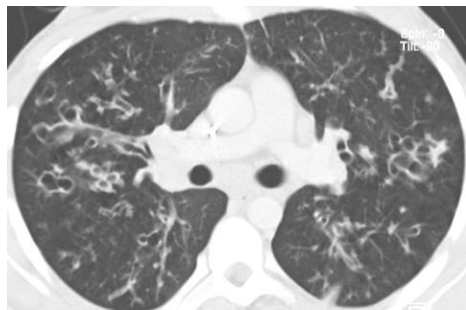
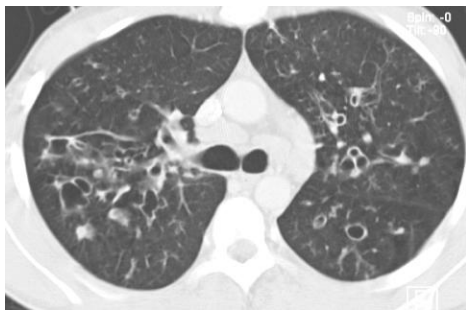
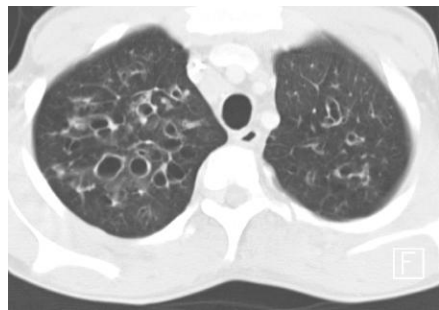
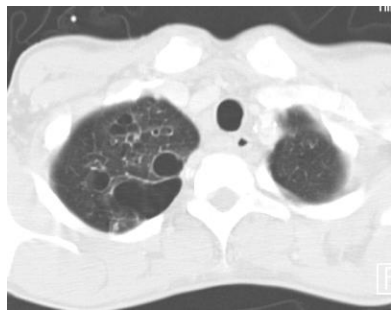
1. Failo R, Wielopolski P, Tiddens H, Hop W, Mucelli R, Lequin M. Lung morphology assessment using MRI: a robust ultra-short TR/TE 2D steady state free precession sequence used in cystic fibrosis patients. Magn Reson Med. 2009 Feb 1;61(2):299–306.

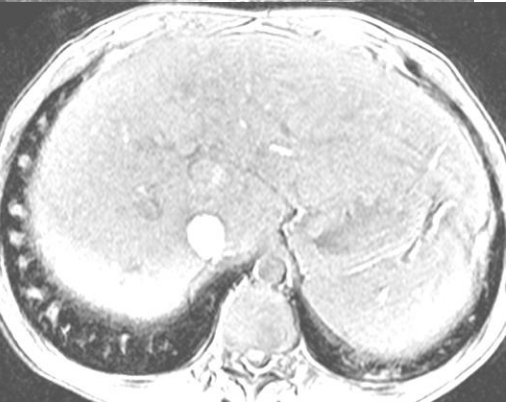
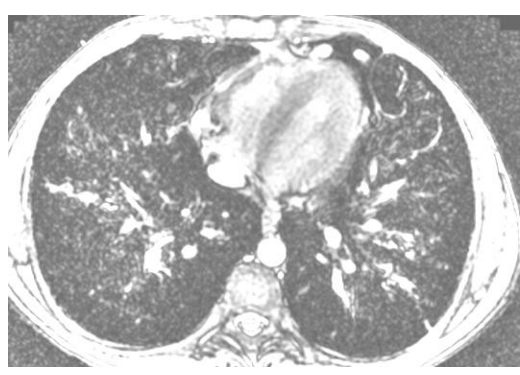
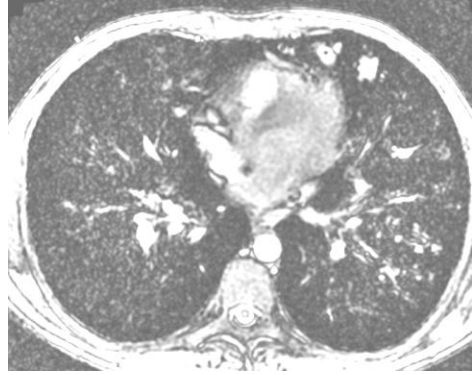
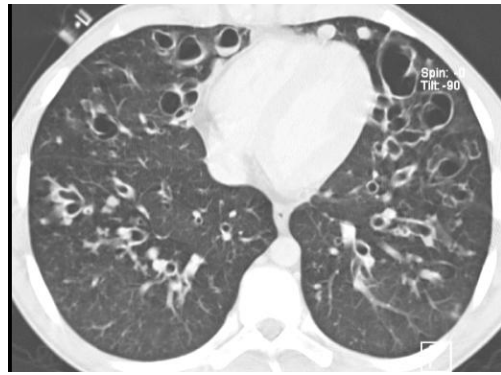
Mucoviscidose

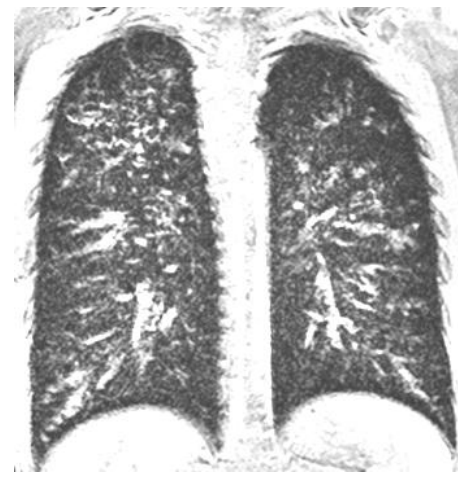
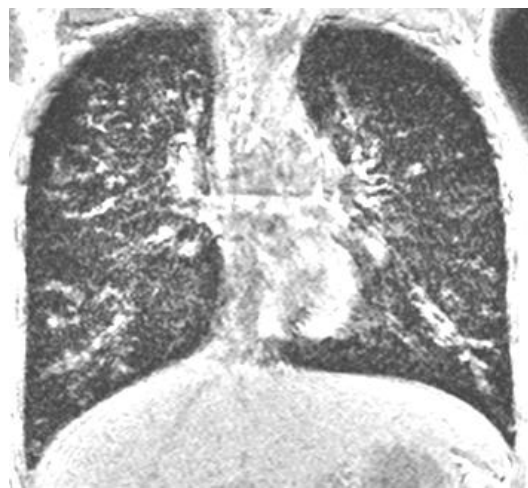
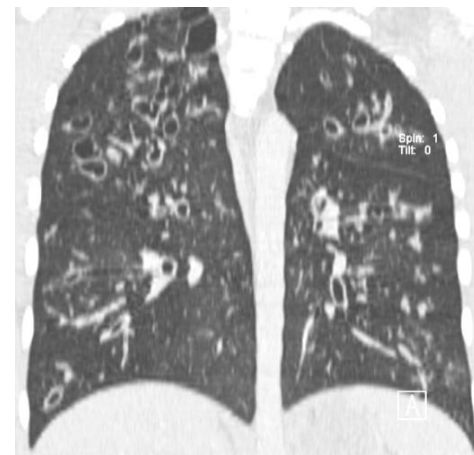
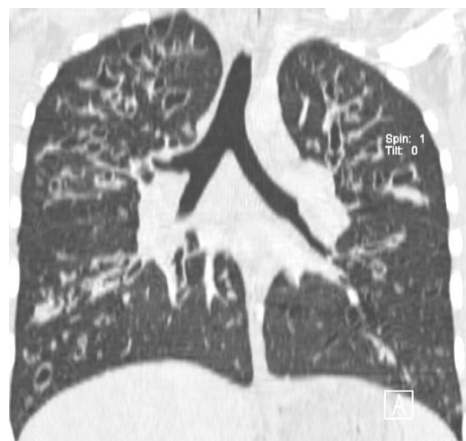
- « Comparaisons » vs CT

- Daltro PA et al. MRI lung findings in pediatric patients with cystic fibrosis compared with CT findings. RSNA 2005
- Hebestreit A et al. Follow-up of acute pulmonary complications in cystic fibrosis by MRI: a pilot study. Acta Paediatr 2004; 93:414-416
- Puderbach M et al. proton MRI appearance of cystic fibrosis: comparison to CT. Eur Radiol 2006









Anomalies parenchymateuses (HTAP)

Table 2

Sensitivity of MR Imaging in the Diagnosis of Various Morphologic Lung Abnormalities and Interobserver Agreement between the Two Readers for MR Imaging

Abnormality	Sensitivity (%)	No. Detected at MR imaging	No. Detected at CT	κ Value*
Pleural effusion	100	15	15	0.89
Pericardial effusion	100	12	12	0.83
Consolidation	100	2	2	0.66
Fibrosis	89	41	46	0.79
Nodules	75	9	12	0.71
Lymph nodes	71	12	17	0.65
Bronchiectasis*	67	4	6	0.61
Atelectasis	64	20	31	0.75
Mucus plugging	50	2	4	0.56
Emphysema	16	7	45	0.60
Mosaic pattern	9	3	33	0.53

* Patients without cystic fibrosis and those with traction bronchiectasis were not included.

Table 3

Overall Accuracy of MR Imaging in the Overall Diagnosis of Pulmonary Fibrosis

Fibrosis	CT Present	CT Absent	Total
MR present	41	3	44
MR absent	5	30	35
Total	46	33	79

Note.—The following values were calculated: sensitivity, 89% (95% CI: 77%, 96%); specificity, 91% (95% CI: 76%, 98%); positive predictive value, 93% (95% CI: 82%, 99%); and negative predictive value, 86% (95% CI: 70%, 95%).

1. Rajaram S, Swift AJ, Capener D, Telfer A, Davies C, Hill C, et al. Lung morphology assessment with balanced steady-state free precession MR imaging compared with CT. *Radiology*. 2012 May;263(2):569–77.

Figure 1



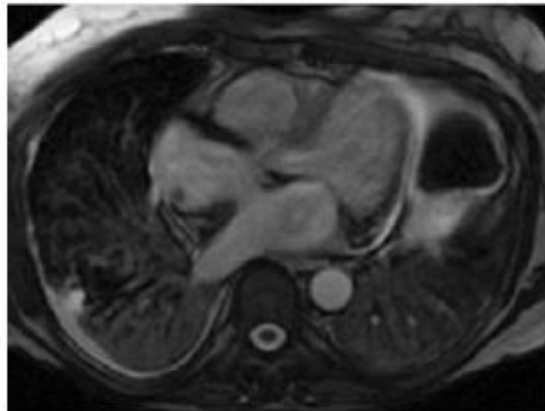
a.



Figure 2



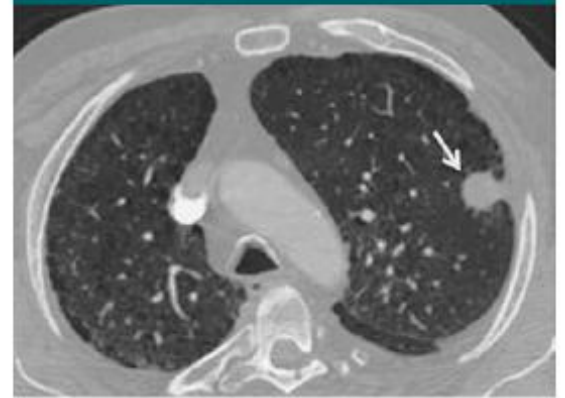
a.



b.

Figure 2: (a) CT and (b) bSSFP MR images show typical nonspecific interstitial pneumonia pattern of

Figure 3



a.



b.

Figure 3: (a) CT and (b) bSSFP MR images show a peripheral 12-mm lung nodule.

Anomalies parenchymateuses (HTAP)

Figure 4

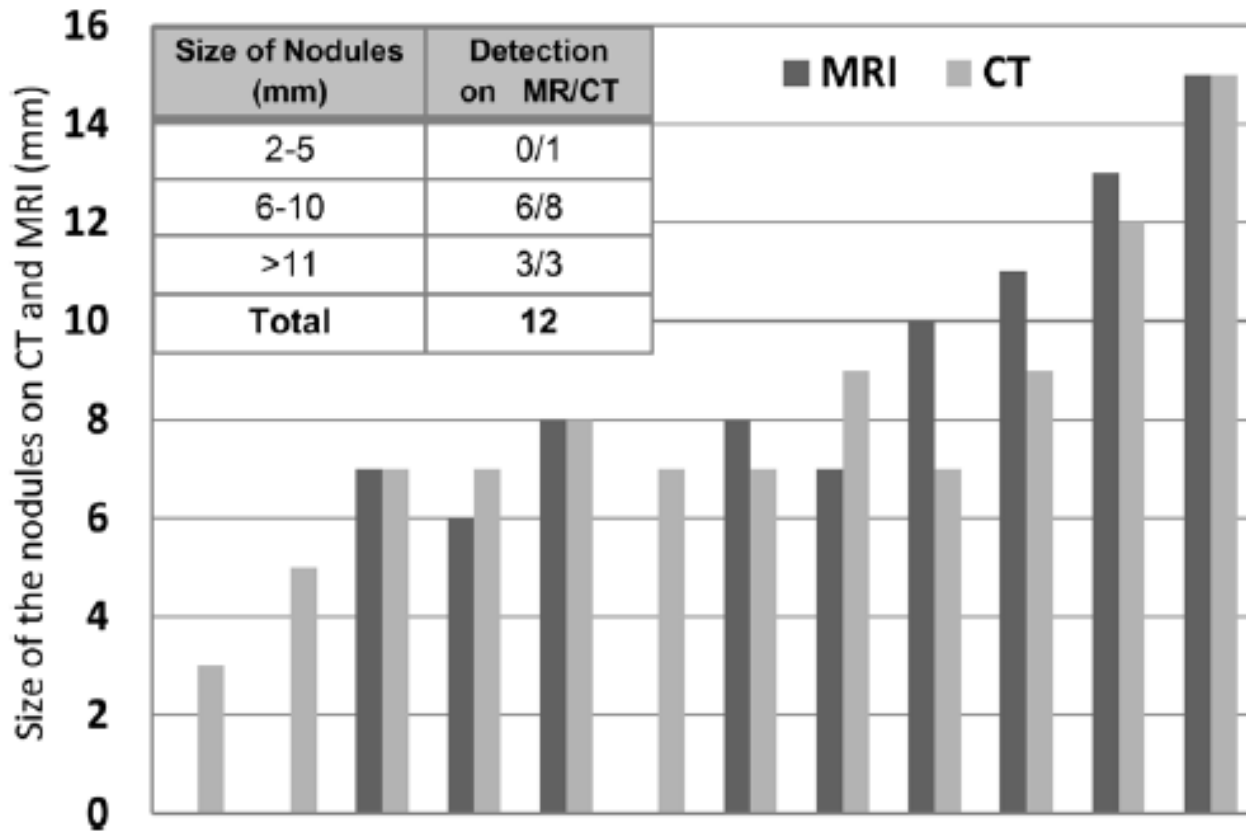
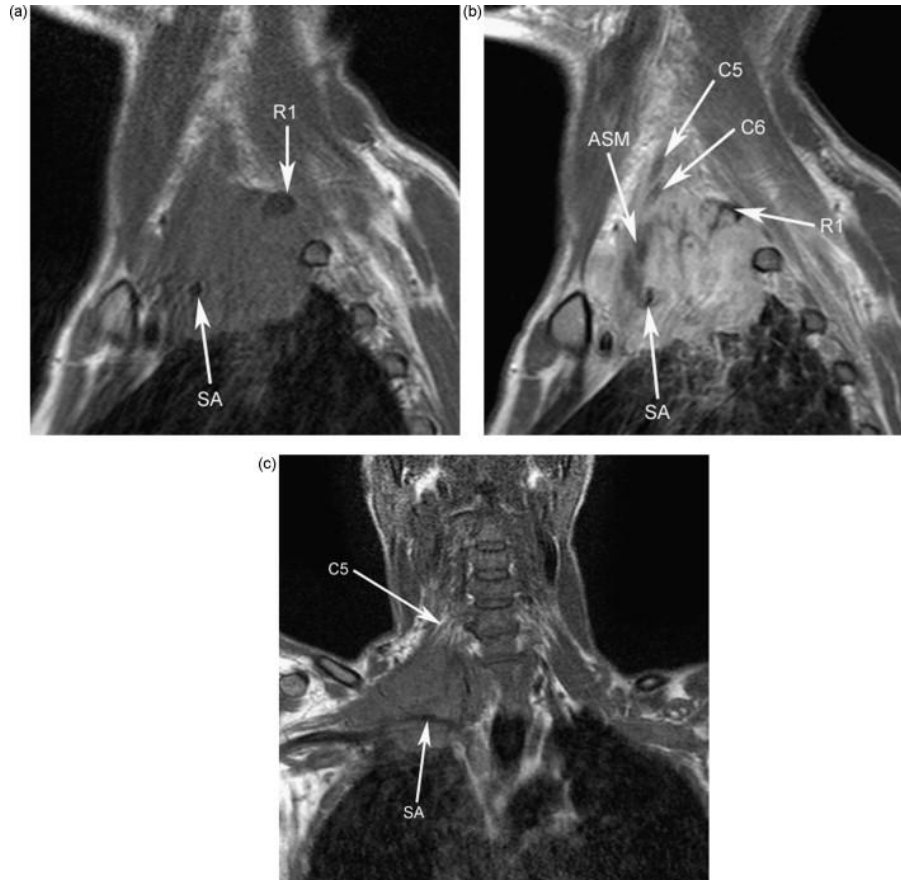


Figure 4: Graph shows detection and size of pulmonary nodules at MR imaging and CT.

1. Rajaram S, Swift AJ, Capener D, Telfer A, Davies C, Hill C, et al. Lung morphology assessment with balanced steady-state free precession MR imaging compared with CT. *Radiology*. 2012 May;263(2):569–77.

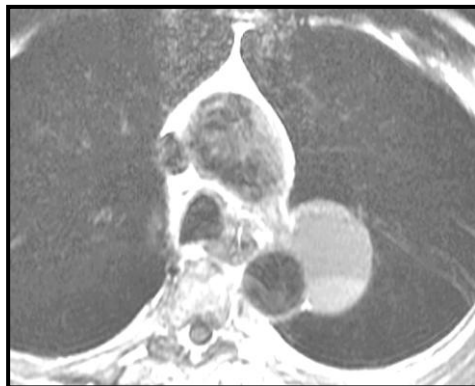
Néoplasie

- Anatomie des tumeurs de l'apex



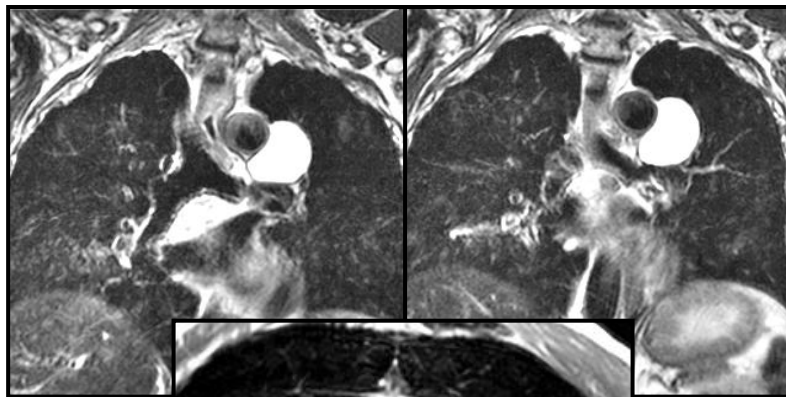
Néoplasie

- Caractérisation tissulaire

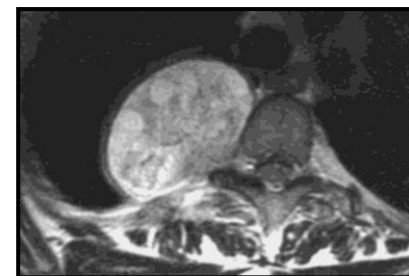
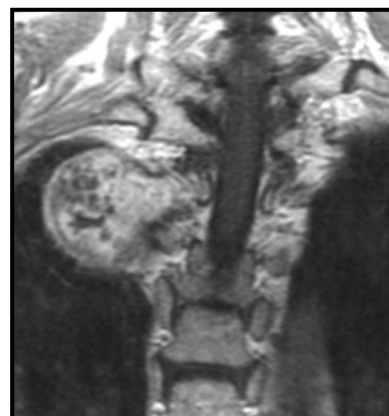
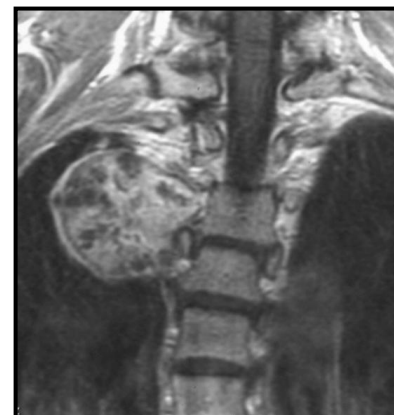
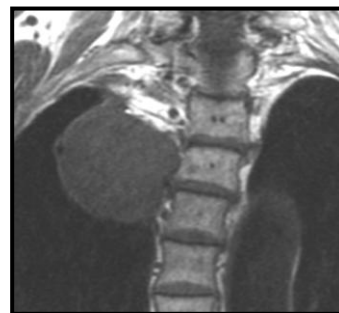


Kyste
bronchogène

pondération T1



pondération
T2



Neurinome dorsal

Staging

Table 2

Tumor Staging Results

Patient No.	TNM Stage at PET/CT	TNM Stage at MR/PET Imaging
1	T1bN0M0	T1bN0M0
2	T2-3N0M0	T2N0M0
3	T3N2M0	T3N2M0
4	T4N2M1b	T4N2M1b
5	T3N0-2M0	T3N0M0
6	T1bN0M0	T1aN0M0
7	T1aN1M0	T1aN1M0
8	T1bN0M0	T1bN0M0
9	T4N2M0	T4N2M0
10	T1aN0M0	T1aN0M0

Note.—Differences in TNM stage were found in patients 2, 5, and 6. TNM stages in patients 3 and 10 are for lesions classified as pneumonia after histologic work-up.

Figure 2

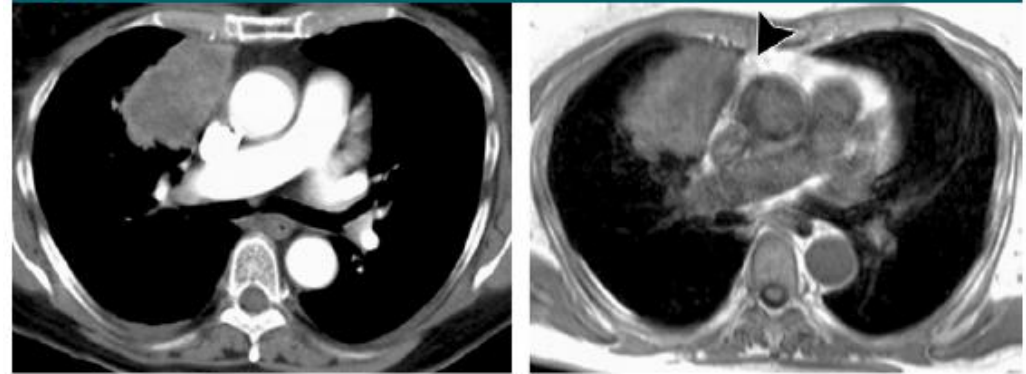
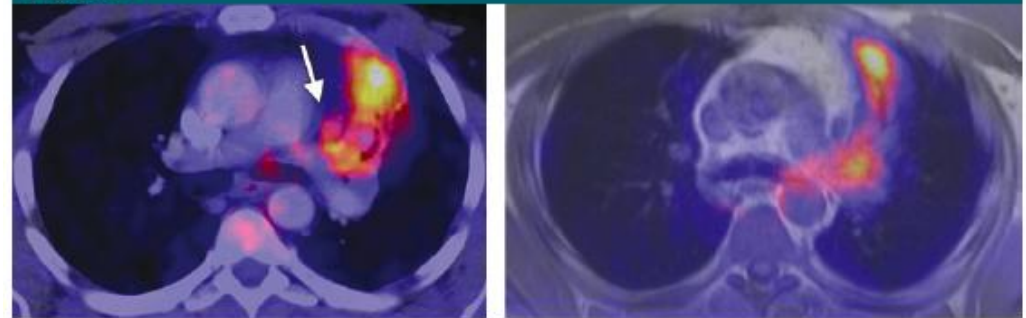


Figure 2: (a) Axial contrast-enhanced CT scan obtained in the arterial phase in patient 2. (b) Axial T1-weighted VIBE MR image in which the prevailing paraaortic fat stripe (arrowhead) is clearly visible.

Figure 3



1. Schwenzer NF, Schraml C, Muller M, Brendle C, Sauter A, Spengler W, et al. Pulmonary Lesion Assessment: Comparison of Whole-Body Hybrid MR/PET and PET/CT Imaging--Pilot Study. *Radiology*. 2012 Jul 20;264(2):551-8.

Staging

N Stage Disease in Patients with Non-Small Cell Lung Cancer:

Efficacy of Quantitative and Qualitative Assessment with STIR Turbo Spin-Echo Imaging, Diffusion-weighted MR Imaging, and Fluorodeoxyglucose PET/CT¹

Ohno et al. Radiology 2011

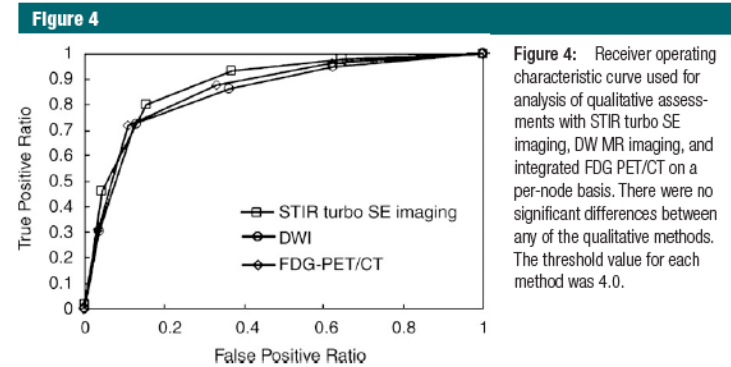
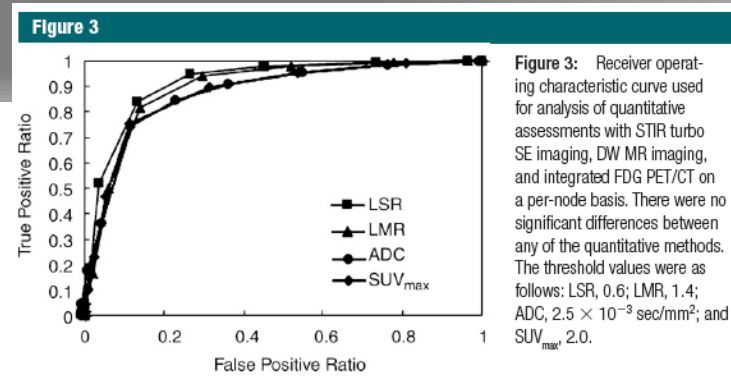
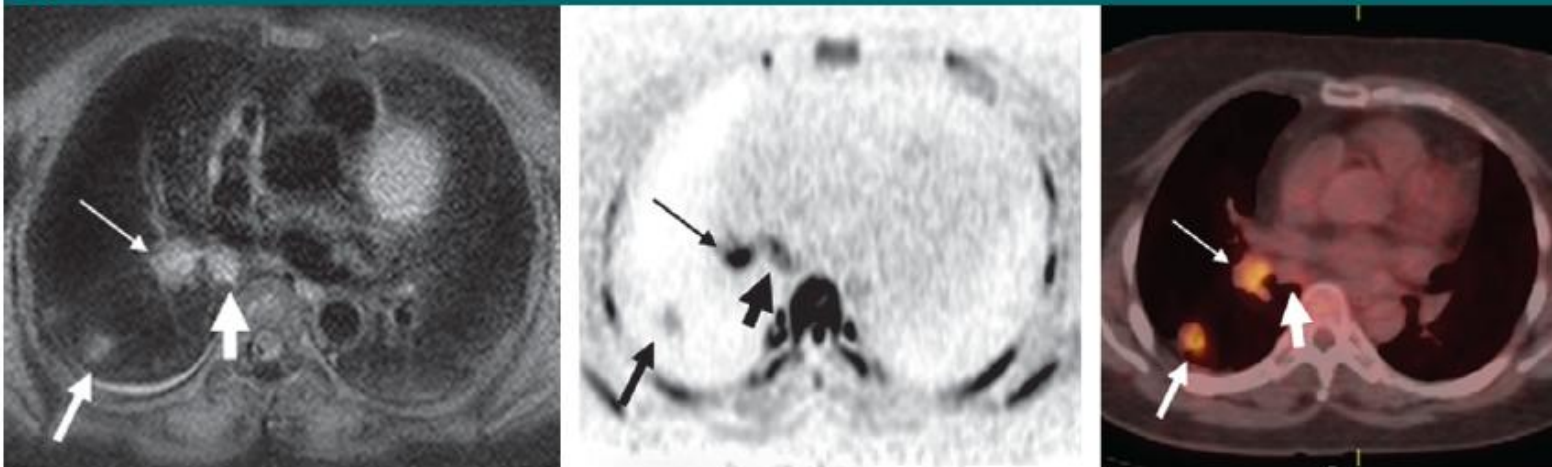


Figure 1

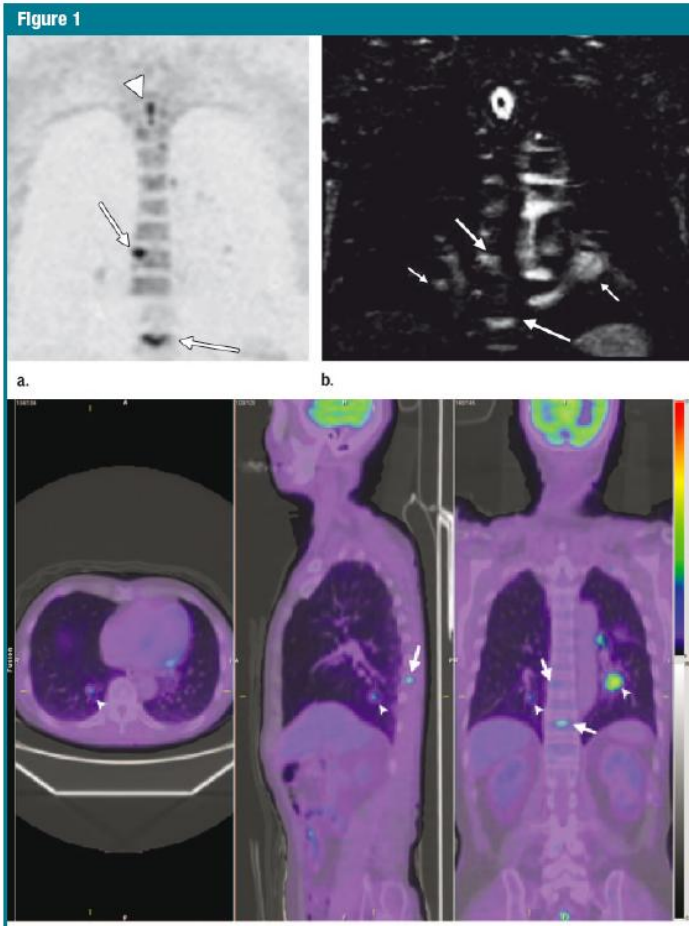


a.

b.

c.

M Staging



1. Ohno Y, Koyama H, Onishi Y, Takenaka D, Nogami M, Yoshikawa T, et al. Non-Small Cell Lung Cancer: Whole-Body MR Examination for M-Stage Assessment--Utility for Whole-Body Diffusion-weighted Imaging Compared with Integrated FDG PET/CT. *Radiology*. 2008 Jul 18;248(2):643-54.

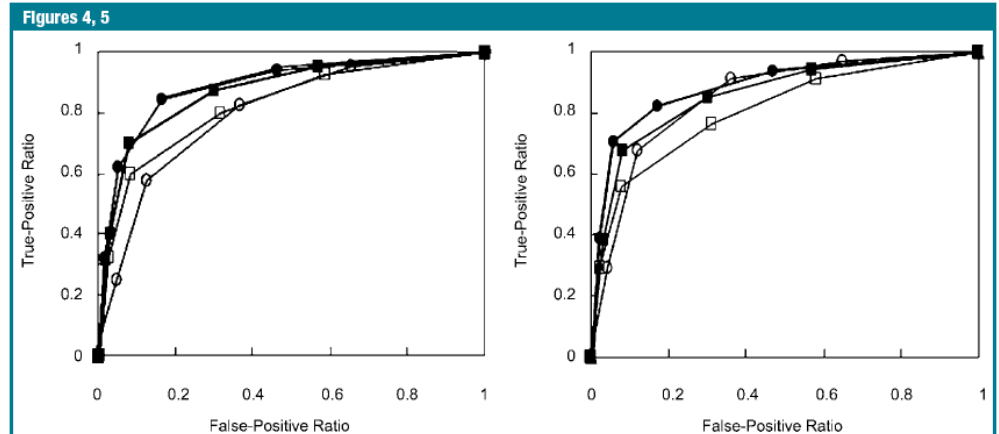
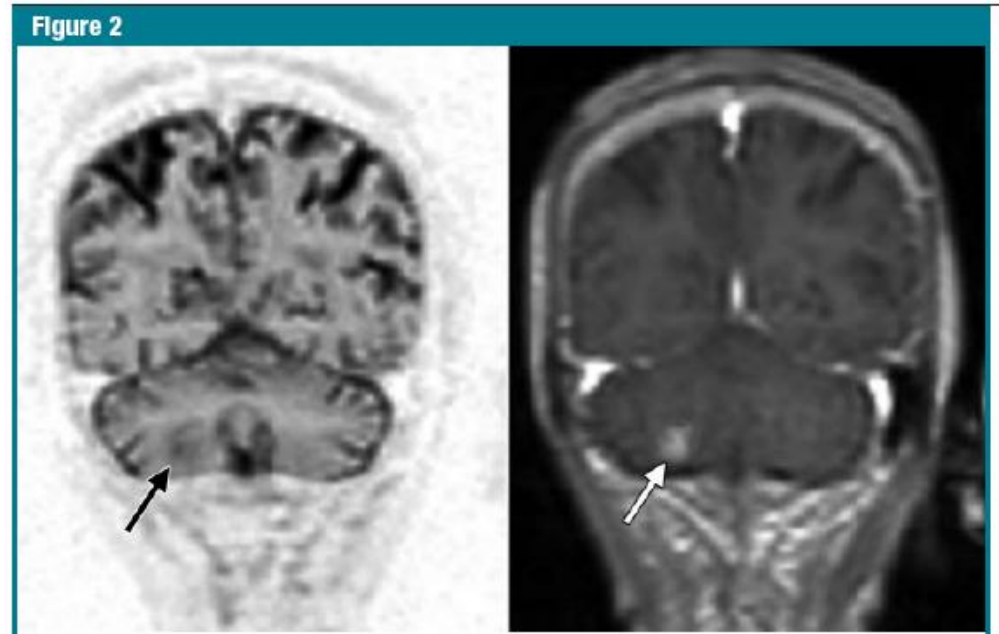
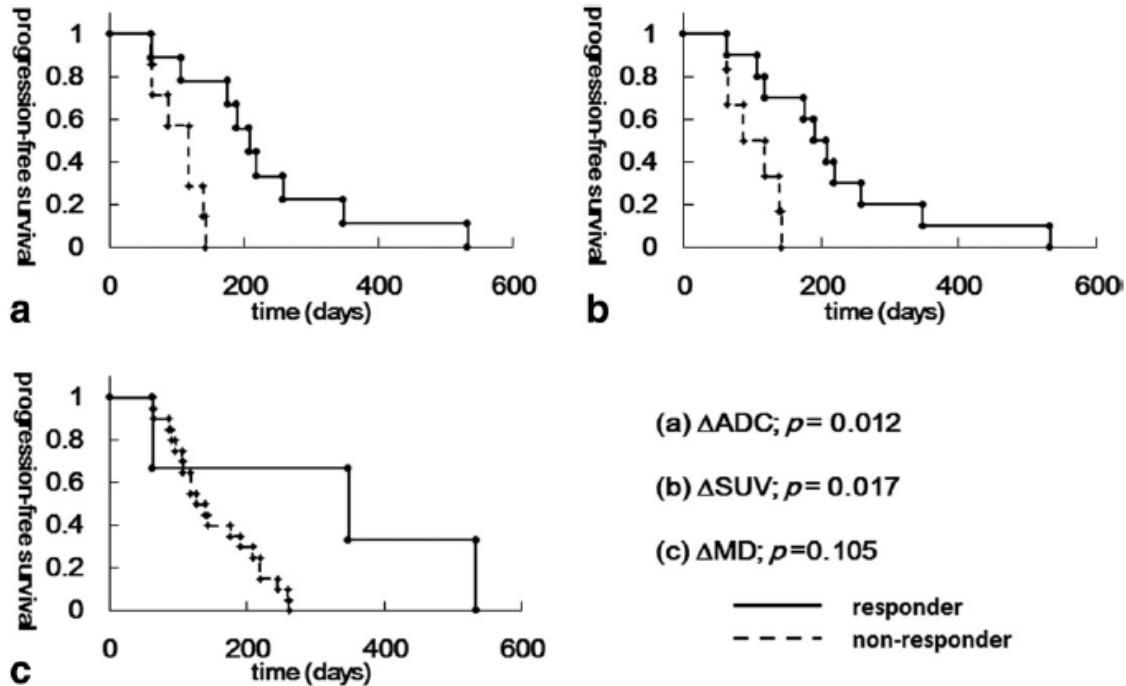


Figure 4: Graph of ROC analyses of whole-body DW imaging (○), whole-body MR imaging with (■) and that without DW imaging (□), and integrated FDG PET/CT (●) for M-stage assessment inclusive of brain metastases on a per-patient basis in patients with NSCLC shows A_z for whole-body MR imaging with DW imaging ($P = .04$) and integrated FDG PET/CT ($P = .02$) as significantly larger than that for whole-body DW imaging.

Figure 5: Graph of ROC analyses of whole-body DW imaging (○), whole-body MR imaging with (■) and that without DW imaging (□), and integrated FDG PET/CT (●) for M-stage assessment exclusive of brain metastases on a per-patient basis in patients with NSCLC shows A_z for integrated FDG PET/CT as significantly larger than that for whole-body MR imaging without DW imaging ($P = .03$).

Réponse au traitement



1. Tsuchida T, Morikawa M, Demura Y, Umeda Y, Okazawa H, Kimura H. Imaging the early response to chemotherapy in advanced lung cancer with diffusion-weighted magnetic resonance imaging compared to fluorine-18 fluorodeoxyglucose positron emission tomography and computed tomography. J Magn Reson Imaging. 2012 Dec 12;;n/a–n/a.

Points clés

- Limites techniques de l'IRM pour l'exploration du parenchyme pulmonaire
- Analyse fonctionnelle non irradiante ?
- Place en oncologie à définir selon évolutions